# Minor contribution of overstory transpiration to landscape evapotranspiration in boreal permafrost peatlands

# Minor contribution of overstory transpiration to landscape evapotranspiration in boreal permafrost peatlands

**Rebecca K Warren**[1,2]**, Christoforos Pappas**[1]**, Manuel Helbig**[1]**, Laura E Chasmer**[3]**, Aaron A Berg**[2]**, Jennifer L Baltzer**[4]**, William L Quinton**[5]**, and Oliver Sonnentag**[1]

[1]Université de Montréal
Département de géographie & Centre d'études nordiques
520 Chemin de la Côte Sainte-Catherine
Montréal, QC, H2V 2B8, Canada

[2]University of Guelph
Department of Geography
50 Stone Road East
Guelph, ON, N1G 2W1, Canada

[3]University of Lethbridge
Department of Geography
4401 University Drive
Lethbridge, Alberta, T1K 3M4, Canada

[4]Wilfrid Laurier University
Department of Biology
75 University Avenue West
Waterloo, ON, N2L 3C5, Canada

[5]Cold Regions Research Centre
Wilfrid Laurier University
75 University Avenue West
Waterloo, ON, N2L 3C5, Canada

Contact Email: rkathwarren@gmail.com

*Submitted to Ecohydrology.*

CONTRIBUTION OF OVERSTORY TRANSPIRATION IN A BOREAL PERMAFROST PEATLAND

1    **Abstract.** Evapotranspiration (ET) is a key component of the water cycle, whereby accurate

2    partitioning of ET into evaporation and transpiration provides important information about the

3    intrinsically coupled carbon, water, and energy fluxes. Currently, global estimates of partitioned

4    evaporative and transpiration fluxes remain highly uncertain, especially for high-latitude

5    ecosystems where measurements are scarce. Forested peat plateaus underlain by permafrost and

6    surrounded by permafrost-free wetlands characterize approximately 60% ($7.0 \times 10^7 \, \text{km}^2$) of

7    Canadian peatlands. In this study, 22 *Picea mariana* (black spruce), a characteristic tree species

8    of the boreal ecozone, were instrumented with sap flow sensors within the footprint of an eddy

9    covariance tower measuring ET of a forest-wetland mosaic landscape. Sap flux density ($J_S$),

10   together with remote sensing and in situ measurements of canopy structure, were used to scale $J_S$

11   to overstory transpiration ($T_{BS}$). Black spruce trees growing in nutrient-poor permafrost peat soils

12   were found to have lower mean $J_S$ than those growing in mineral soils and contribute less than

13   1% to landscape ET. Climate change-induced forest loss and the expansion of wetlands may

14   further minimize the contributions of $T_{BS}$ to ET, and increase the contribution of standing water.

15

## 1. Introduction

17   Evapotranspiration (ET) is a key component of the water cycle and can be partitioned into biotic

18   and abiotic components (e.g., Wang and Dickinson (2012)). The former consists of transpiration,

19   i.e., the loss of water primarily from plant stomata, while the latter encompasses evaporation

20   from plant interception, soil and open water evaporation, as well as snow sublimation (Lawrence

21   *et al.*, 2007; Fatichi and Pappas, 2017). Accurate partitioning of ET into evaporation and

22   transpiration components provides important information to validate and improve the simulation

23   of carbon, water, and energy fluxes within terrestrial ecosystem models (Lawrence *et al.*, 2007;

CONTRIBUTION OF OVERSTORY TRANSPIRATION IN A BOREAL PERMAFROST PEATLAND

24  Wang and Dickinson, 2012; Fatichi *et al.*, 2015; Fatichi and Pappas, 2017). Increasingly,

25  accurate partitioning of water fluxes at regional scales are also required to reliably quantify and

26  manage water resources under rapidly changing climatic and environmental conditions (Bonan,

27  2008; Schaefer *et al.*, 2012). Numerous studies have partitioned ET into its component fluxes

28  (e.g., Jasechko *et al.* (2013), Good *et al.* (2015)). However, global estimates remain highly

29  uncertain (e.g., Coenders-Gerrits *et al.* (2014), Wang *et al.* (2014)). Moreover, most of the global

30  scale analyses focus on temperate regions, with ET partitioning in northern boreal and high-

31  latitude ecosystems remaining under-represented due to limited available information (e.g., Good

32  *et al.* (2015),  Jasechko *et al.* (2013), Schlesinger and Jasechko (2014), Fatichi and Pappas

33  (2017)).

34       Peatlands are found throughout the boreal biome and are defined as ecosystems with

35  more than 40 cm of accumulated organic material. Distinct peatland classes can be defined based

36  on their hydrology, vegetation, and chemical composition (National Wetlands Working Group,

37  1997), and further described by the presence or absence of permafrost, i.e., perennially cryotic

38  ground (Zoltai and Tarnocai, 1975). Peatlands of high boreal and low subarctic regions comprise

39  58% of the total peatland area in Canada (Figure 1b). Such high-latitude peat landscapes are

40  often characterized by forested permafrost peat plateaus that are elevated approximately 1 m

41  above surrounding wetlands, mostly patterned and/or flat fens, and collapse-scar and/or flat bogs

42  (Zoltai and Tarnocai, 1975). Permafrost only occurs under peat plateaus, being absent from

43  adjacent fens and bogs.

44       Climate change-induced permafrost thaw could potentially to influence boreal and

45  subarctic peatland land-surface interactions at the regional scale (Grosse *et al.*, 2016). Along its

46  southern limit, permafrost is relatively warm and thin (Smith *et al.*, 2005). In recent decades,

3

CONTRIBUTION OF OVERSTORY TRANSPIRATION IN A BOREAL PERMAFROST PEATLAND

47  warming air temperatures have accelerated the rate of permafrost thaw (Baltzer *et al.*, 2014;

48  Chasmer and Hopkinson, 2016; Grosse *et al.*, 2016; Quinton *et al.*, 2011) impacting forest

49  composition, structure and function (Baltzer *et al.*, 2014; Jorgenson *et al.*, 2013; Lara *et al.*,

50  2016), and thus carbon, water and energy fluxes (Grosse *et al.*, 2016; Helbig *et al.*, 2016b;

51  Turetsky *et al.*, 2002). Thawing sporadic discontinuous permafrost, i.e., permafrost occurring on

52  <50% of the landscape, has been shown to induce surface subsidence, thereby replacing forests

53  (i.e. peat plateaus) with permafrost-free wetlands (referring to fens and bogs in this study)

54  (Baltzer *et al.*, 2014; Jorgenson *et al.*, 2013; Lara *et al.*, 2016). The post-thaw wetland water

55  table is close to the ground surface allowing open water or energy-limited ET, in contrast to the

56  raised peat plateaus that are water-limited. Land cover conversion from mostly black spruce

57  dominated peat plateaus with permafrost to treeless, permafrost-free wetlands may therefore

58  increase landscape ET across parts of northwestern Canada (Helbig *et al.,* 2016b).

59      Here, we use tree-level sap flux density measurements ($J_S$; i.e., sap flow per unit of

60  sapwood area) of black spruce, a widespread boreal tree species, together with site-specific tree

61  allometry and a canopy height model (CHM) derived from Light Detection and Ranging

62  (LiDAR) to estimate overstory transpiration over a boreal peat landscape with sporadic

63  permafrost in northwestern Canada. Upscaled overstory transpiration is then compared with

64  landscape ET estimates from concurrent eddy covariance measurements. The objectives of this

65  study are (i) to quantify the contribution of black spruce transpiration ($T_{BS}$) to landscape ET, and

66  (ii) to discuss the impacts of a shift in $T_{BS}$/ET as a result of permafrost thaw-induced boreal

67  forest loss and wetland expansion.

68

69  **2. Materials and methods**

4

CONTRIBUTION OF OVERSTORY TRANSPIRATION IN A BOREAL PERMAFROST PEATLAND

70    *2.1. Study site*

71    The study site is a boreal forest stand of *ca.* 0.75 km$^2$ on permafrost peat plateaus with

72    interspersed permafrost-free bogs and fens, situated in the southern portion of the Scotty Creek

73    watershed, Northwest Territories (NT), Canada (61.17'83°N, 121.17'25°W) (Figure 1a). Scotty

74    Creek is a hydrologically well-characterized watershed south of Fort Simpson, NT under the

75    influence of rapidly thawing sporadic permafrost (Quinton *et al.*, 2011). The climate of the

76    region is characterized by short summers and long, cold winters with a mean annual air

77    temperature and a total precipitation of -2.8 °C and 390 mm, respectively (1981 – 2010 climate

78    normals, Fort Simpson, Environment Canada, 2014).  Mean annual air temperature has increased

79    since the 1970's, contributing to accelerated permafrost thaw increasing from 0.19% (of total

80    basin area) per year (1970 - 2000) to 0.58% per year (2000 - 2015) (Chasmer and Hopkinson,

81    2016). The increasing rate of permafrost disappearance has caused expansion of bogs and fens at

82    the expense of forested peat plateaus at Scotty Creek, and across the southern Taiga Plains

83    ecozone (Baltzer *et al.*, 2014; Chasmer and Hopkinson, 2016; Helbig *et al.*, 2016b). Similar

84    landscapes to Scotty Creek are widespread throughout the Canadian and Russian boreal ecozone

85    (Olefeldt *et al*, 2016), with a reported 21% of the global boreal forest classified as lowland forest

86    overlying permafrost or thick overburden (Helbig *et al*, 2016a).

87         Forested permafrost peat plateau vegetation consists of a *Picea mariana* (black spruce)

88    dominated overstory and sporadic *Larix laricina* (tamarack), which combined constitute >95% of

89    stems >1 cm (J L Baltzer, *unpublished data*). *Picea glauca* (white spruce), *Pinus banksiana* (jack

90    pine), *Populus tremuloides* (trembling aspen), and *Betula neoalaskana* (Alaskan paper birch)

91    also occasionally occur. The understory is composed of *Betula spp.* (birch) shrubs,

92    *Rhododendron groenlandicum* (bog Labrador tea), *Andromeda polifolia* (bog rosemary), *Cladina*

5

93   *spp.* (reindeer lichen), *Pleurozium schreberi* (feather moss) and *Sphagnum spp.* (Garon-

94   Labrecque *et al.*, 2015). The average tree height (*H*) is 2.2 m ± 1.2 and stand density is *ca.* 0.12

95   stems m$^{-2}$ (peat plateaus = 0.18 stems m$^{-2}$, bogs = 0.07 stems m$^{-2}$, fens = 0.03 stems m$^{-2}$), as

96   extracted from the CHM. As the CHM does not differentiate between different tree species, all

97   trees were assumed to be black spruce, which dominate the landscape (*ca.* 83%, J L Baltzer,

98   *unpublished data*). Leaf Area Index (LAI; LAI-2200 Plant Canopy Analyzer, Li-COR

99   Biosciences, Lincoln, NE, USA) was estimated (Sonnentag *et al.*, 2007) for over- (0.61 m$^2$ m$^{-2}$ ±

100   0.34 (one standard deviation)) and understory (0.68 m$^2$ m$^{-2}$ ± 0.25) vegetation (*n* = 31), in July

101   2013. Ericaceous shrubs and *Sphagnum spp.* generally dominate bogs, while shrubs, sedges,

102   grasses, and brown mosses dominate fens (Garon-Labrecque *et al.*, 2015).

103

104   *2.2. Sap flux density measurements*

105   During a portion the 2013 growing season (May 31 to July 13), 22 black spruce trees of similar

106   size (10.0 - 11.9 cm diameter at breast height) were instrumented at breast height (1.3 m) with

107   heat-ratio-method sap flow sensors (HRM; SFM1 Sap Flow Meter, ICT International, Armidale,

108   New South Wales, Australia; following Burgess *et al.* (2001)). All trees were located in the

109   interior of peat plateaus, avoiding edges where tree function has been shown to be reduced

110   (Patankar *et al.*, 2015). These trees were selected to span the range of environmental conditions

111   (e.g. nutrient gradient) present at Scotty Creek and thus capture within-site variability in sap

112   flow.  Most of the instrumented trees were located within or near the landscape eddy covariance

113   flux tower footprint (Figure 1a). Heat pulse sap velocity (*V*$_S$, cm hr$^{-1}$) was calculated from the

114   Sap Flow Tool software (ICT International Armidale, New South Wales, Australia). Sap velocity

115   measured at the first thermistor (length equal to 12.5 mm) was used in our study, as the second

116    thermistor (length equal to 27.5 mm) was located in non-conducting wood tissues (heartwood).

117    $J_S$ (gH$_2$O m$^{-2}$ s$^{-1}$) was derived from $V_S$ every 30 minutes, assuming one unit of sapwood area and

118    water density was equal to 1000 kg m$^{-3}$.

119

120    *2.3. Eddy covariance and supporting measurements*

121    Boreal forest-wetland "landscape" ET (ET$_{LAND}$; 2013 – 2016) and "wetland" ET (ET$_{BOG}$; 2014 –

122    2016) were obtained from nested eddy covariance measurements (Helbig *et al.*, 2016b), installed

123    in August 2012 and 2013 respectively. Two towers were equipped with the same flux and

124    micrometeorological instrumentation, including an infrared CO$_2$/H$_2$O gas analyzer (EC150;

125    Campbell Scientific Inc., Logan, UT, USA) and a three-dimensional sonic anemometer

126    (CSAT3A; Campbell Scientific Inc.). These were mounted on a 15-m tower located on the

127    forested peat plateau, and approximately 100 m north at the bog site on a 2 m tripod,

128    respectively. A detailed description of the eddy covariance set-up at Scotty Creek is given by

129    Helbig *et al.* (2016b). The 90% landscape and bog flux footprints were derived from a 2D

130    footprint parameterization (Kljun *et al.*, 2015), which were used to quantify the mean growing

131    season ET flux footprint contributions from forested peat plateaus ($a$ = 51 %) and wetlands ($b$ =

132    49 %) (see equation 1 below). For the landscape tower, all fluxes within the footprint with >5%

133    contributions from the lake were filtered. Contributions from fens never exceeded 10%, and were

134    aggregated with the bog contribution for a total wetland flux. For the wetland tower, all fluxes

135    with contribution greater than 5% from the forest were similarly filtered. To estimate ET$_{BOG}$ for

136    2013, when only ET$_{LAND}$ and sap flux density were measured, we applied a linear relationship

137    between concurrent ET$_{LAND}$ and ET$_{BOG}$ measurements during the other years following Helbig *et*

138    *al,* (2016b). We used the mean slope and intercept for the three-year period: 1.26 ± 0.18 and -

7

139  $1.68 \pm 0.24$ mg $H_2O$ m$^{-2}$ s$^{-1}$ ($n = 3$), respectively (see Supplementary material Figure S1).

140  Measured $ET_{LAND}$ in 2013 was then partitioned to derive forest (i.e., peat plateau) ET ($ET_{FOR}$)

141  using the mean weighted flux footprint contributions for the two land cover types (forest [FOR]

142  and wetland [BOG]) and the derived $ET_{BOG}$:

$$ET_{LAND} = a ET_{FOR} + b ET_{BOG} \tag{1}$$

143  Photosynthetically active radiation (PAR, µmol m$^{-2}$ s$^{-1}$; PQS1, Kipp and Zonen, Delft, the

144  Netherlands), vapour pressure deficit (VPD, hPa; Rotronic AG, Bassersdorf, Switzerland), and

145  air temperature (°C; HC2-S3, Rotronic AG, Bassersdorf, Switzerland) were measured at the

146  landscape tower above the forest canopy at 30-minute intervals. Precipitation (mm) was also

147  measured at 30-minute intervals using a tipping bucket rain gauge (TR-5251, Texas Electronics

148  Inc., Dallas, Texas, USA) located within the landscape flux footprint.

149

150  *2.4. Allometric relationships*

151  Allometric field surveys in the landscape flux footprint were conducted in 2012 ($n = 100$), 2015

152  ($n = 51$) and 2016 ($n = 47$) to establish the relationship between black spruce $H$ (m) and DBH

153  (cm). Both $H$ and DBH were non-normally distributed and heteroscedastic, and therefore

154  subsequently log-transformed. A site-specific relationship (Figure 2) was developed to relate $H$

155  and DBH (DBH = $10^{0.067} \times H^{0.989}$, r$^2$ = 0.67, p < 0.001, $n = 198$). A correction factor of 1.054

156  was applied to account for the systematic bias to the base logarithm introduced by the log-

157  transformation (Sprugel, 1983).

158

159  The allometric relationship between DBH and sapwood area ($A_S$, cm$^2$) was similarly log-

160  transformed using data from the 2016 survey. Sapwood thickness was identified visually after

8

161 examining tree cores against the sunlight (mean 10.0 mm +/- 6.1, $n$ = 47). Sapwood was

162 relatively wet and translucent in comparison to heartwood. This relationship was best described

163 by the function $A_S = 10^{-0.633} \times DBH^{1.848}$ ($r^2$ = 0.76, p < 0.001) with a correction factor of 1.059

164 (Figure 2b).

165

166 *2.5 Upscaling tree-level sap flux density to landscape evapotranspiration*

167 A LiDAR dataset of Scotty Creek at 1 $m^2$ spatial resolution was acquired in 2010 and used to

168 produce a CHM (Chasmer *et al.*, 2014; Chasmer *et al.*, 2011). Grid cells with canopy heights <1

169 m were excluded from the analysis as these represent understory and ground surface vegetation

170 structures. Per 1 $m^2$ CHM grid cell, sap flux density was scaled from individual tree- ($J_S$) to

171 overstory- ($T_{BS}$), and thus landscape-level, based on the equation:

$$T_{BS} = J_S \frac{A_S}{A_G} \qquad (2)$$

172 where $J_S$ is the average half-hourly sap flux density ($gH_2O$ $m^{-2}$ 30 $min^{-1}$), $A_S$ is the sapwood area

173 per grid cell ($m^2$), and $A_G$ is the grid cell area ($m^2$). We assume a maximum stem density of one

174 tree per $m^2$, i.e., a CHM cell cannot contain more than one individual, which is supported by a

175 stand density of <1 stem $m^{-2}$. Sapwood area was calculated from the footprint-specific allometric

176 relationships between $H$, DBH, and $A_S$ using the CHM. To address potential uncertainties in

177 sapwood depth measurements in resinous tree species (e.g., Van Herk *et al.* (2011)), we

178 examined also an hypothetical scenario where $A_S$ equalled the cross-sectional area ($A_{CS}$) for trees

179 with a DBH ≤ 5.4 cm (i.e., the average of the studied trees in Van Herk *et al.* (2011)) and $A_S$ =

180 $0.5A_{CS}$ for trees with a DBH ≥ 5.4 cm. This approach allowed us to obtain an upper limit of

181 scaled $T_{BS}$ and of its contribution to $ET_{LAND}$.

182

9

CONTRIBUTION OF OVERSTORY TRANSPIRATION IN A BOREAL PERMAFROST PEATLAND

183  *2.6 Uncertainty analysis*

184  Possible sources of uncertainty in $T_{BS}$ are (i) an underestimation of $H$ from the CHM due to

185  low/no returns from the apices of narrow black spruce crowns, (ii) uncertainties in the derived

186  allometric equations, and (iii) variability of $J_S$ between trees. These uncertainties were addressed

187  using a Monte Carlo uncertainty analysis (MC-UA) of the scaling procedure. LiDAR-derived

188  canopy height was assumed to be approximately 10% lower than measured tree height as found

189  by Hopkinson *et al.* (2005). The CHM uncertainties were implemented in the MC-UA by

190  replacing each grid cell value with a canopy height sampled from a normal distribution with

191  mean equal to the original CHM value of this grid cell and standard deviation of 10%. The

192  allometric relationships derived in Figure 2 were applied to the CHM to estimate transpiration

193  fluxes from the area within the flux footprint, and included the range of error associated with

194  underestimated canopy height (see Supplementary Material Figures S3-6). Uncertainties arising

195  from using mean $J_S$ were addressed by randomly sampling from a normal distribution with the

196  standard deviation of $J_S$ from all instrumented trees per time step. Per MC-UA iteration (100 in

197  total), $T_{BS}$ was calculated for each CHM grid cell using equation 2 and summed to determine

198  total footprint $T_{BS}$. Black spruce transpiration for the footprint is given as the mean $T_{BS}$ of the

199  iterations +/- the standard deviation.

200

201  **3. Results and discussion**

202  *3.1. Daily and seasonal patterns of sap flux density*

203  Total precipitation at Scotty Creek during the study period (May 31 to July 13 2013) amounted

204  to 88.8 mm, with mean air temperature of 17.6 °C (minimum = 4.1 °C, maximum = 32.2 °C)

205  (Figures 3a,f). Maximum air temperature and VPD occurred late-June to early-July, while

206   maximum PAR was observed early-June to early-July (Figures 3d-f). Black spruce $J_S$ was

207   greater than zero throughout the day, most likely due to the long photoperiod (~22 h) (Patankar

208   *et al.* 2015; Figures 3b-e) . Maximum $J_S$ occurred approximately a month after snowmelt in

209   early-May (Connon *et al.*, 2015) and slowly declined over the remainder of the growing season,

210   with the exception of days following rainfall (Figures 3a,b). On days with larger precipitation

211   events (Figure 3a), $J_S$ approached zero and differed from the typical diurnal pattern (Figure 3b).

212   A similar daily and seasonal flux pattern was observed for $ET_{LAND}$ (Figure 3c).

213        In comparison to previous black spruce sap flux density studies (Table 1), black spruce at

214   Scotty Creek had lower mean daily $J_S$ (minimum = 0.1, mean = 8.0, maximum = 21.7 in $gH_2O$

215   $m^{-2}$ $s^{-1}$). Angstmann *et al.* (2013) found similarly low mean daytime $J_S$ in black spruce growing

216   in peat soils. In contrast, $J_S$ reported for smaller-DBH black spruce growing in mineral soils were

217   about ten times higher (Ewers *et al.*, 2005; Van Herk *et al.*, 2011). This difference may be due to

218   a number of environmental factors controlling the magnitude of $J_S$, including stand structure

219   (Angstmann *et al.*, 2012; Ewers *et al.*, 2005), moisture gradients (Angstmann *et al.*, 2013;

220   Bovard *et al.*, 2005; Oren and Pataki, 2001), soil nutrients, and presence or absence of

221   permafrost (Iijima *et al.*, 2014; Patankar *et al.*, 2015). In particular, Scotty Creek has the lowest

222   overstory LAI, canopy height and stand density among the reported studies in Table 1, and is

223   additionally underlain by nutrient-poor, peat soils. Low nitrogen availability of similar black

224   spruce forests growing on permafrost-affected peat soils in Alaska has been recently reported

225   Finger *et al.* (2016). Additionally, black spruce rooting depth is commonly limited to the top 20

226   cm of soil (Finger *et al.*, 2016; Gale and Grigal, 1987) controlling access to water as the growing

227   season progresses (Patankar *et al.*, 2015; Sniderhan and Baltzer, 2016). It should also be noted

228   that $J_S$ may also vary depending on measuring technique, e.g. HRM (this study), versus Granier-

CONTRIBUTION OF OVERSTORY TRANSPIRATION IN A BOREAL PERMAFROST PEATLAND

229  style sensors (Table 1) and/or data corrections applied *a posteriori* to account for possible

230  contact of the sap flow probes with non conductive tissues (e.g., Steppe *et al.* (2010)).

231

*3.3. Evapotranspiration and black spruce transpiration*

233  Mean daily $ET_{LAND}$ (+/- one standard deviation) per m$^2$ of the footprint in 2013 was 2.33 mm d$^{-1}$

234  +/- 0.77 and was partitioned into $ET_{FOR}$ = 1.72 mm d$^{-1}$ +/- 0.57 and $ET_{BOG}$ = 2.92 mm d$^{-1}$ +/-

235  0.97. Mean daily $T_{BS}$ was 0.02 mm d$^{-1}$ +/- <0.01 composed of 0.03 mm d$^{-1}$ +/- 0.01 from forested

236  areas (i.e., peat plateaus, $T_{BS-FOR}$) and <0.01 mm d$^{-1}$ from wetlands ($T_{BS-BOG}$). Overall, $T_{BS}$

237  contributed 0.9 % to $ET_{LAND}$ (1.9% to $T_{BS-FOR}$ and 0.4 % to $T_{BS-BOG}$; Figure 4). The upper limit of

238  $T_{BS}$ and of its contribution to $ET_{LAND}$ indicated that $T_{BS}$ may account for up to 2.1% of $ET_{LAND}$,

239  and $T_{BS-FOR}$ for 4.5% of $ET_{FOR}$; however, $T_{BS}$ remains a minor contribution to ET. These findings

240  suggest that black spruce forests growing on peat soils, especially with permafrost, may

241  contribute much less to ET than their mineral soil counterparts (Table 1). In contrast to sites with

242  greater canopy coverage, the sparse tree density at Scotty Creek allows plenty of light to

243  penetrate into the black spruce canopy and to reach the understory layer (Chasmer *et al.*, 2011),

244  potentially allowing understory transpiration (i.e. Labrador tea, birch, moss, lichen) to play a

245  larger role in the landscape water balance (Lafleur, 1992).

246

*3.3. Climate change and evapotranspiration in boreal permafrost peatlands*

248  Accelerated rates of permafrost thaw, and continued climate warming have already resulted in

249  landscape changes through forest loss and the expansion of wetlands along the southern limit of

250  permafrost (Baltzer *et al.*, 2014; Helbig *et al.*, 2016a).  For example, the recent study of Chasmer

251  and Hopkinson (2016) projects a complete loss of permafrost from the Scotty Creek basin by *ca.*

252    2044. Helbig *et al.* (2016b) found that with permafrost thaw-induced wetland expansion the

253    partitioning of available energy will shift from sensible heat flux more toward to latent heat flux

254    and thus ET, as the flux from a bog-only flux footprint is 1.54 times greater than the landscape

255    flux footprint (ca. 50% wetland and ca. 50% forest). Continued wetland expansion across these

256    regions would increase $ET_{LAND}$, mainly due to an increase in open water and moss evaporation,

257    and even further minimize the contribution of black spruce to the water balance. Additionally,

258    root sap flux density has been shown to be significantly lower in black spruce trees near peat

259    plateau edges in the peat plateau-wetland transition zone compared with interior peat plateau

260    trees (Baltzer *et al.*, 2014; Patankar *et al.*, 2015). Thus, it may be surmised that with the increase

261    in both wetland expansion and forest fragmentation, combined with growth reductions that have

262    been attributed to active layer thickening (Sniderhan and Baltzer, 2016), the contribution of $T_{BS}$

263    to $ET_{LAND}$ will even further decrease. However, in contrast to other forested systems, loss of

264    trees in a permafrost boreal peat landscape likely does not directly alter landscape ET, or account

265    for the observed increase in basin runoff, attributed to the increasingly interconnected wetland

266    features (Connon *et al.*, 2014) that promote ET. Additionally, while forest loss is not likely to

267    significantly alter water fluxes directly, the associated collapse of peat plateaus with permafrost

268    thaw is expected to increase water availability to the moss surface and enhance total evaporation,

269    as demonstrated by the systematic difference in $ET_{LAND}$ and $ET_{BOG}$ in this study, and the findings

270    of Helbig *et al.* (2016b). Increased drainage and a future drier state in this system may permit the

271    recovery of forests, and potentially enhance the contribution of overstory transpiration to ET.

272

273    **4. Conclusion**

274    In this study, we quantified the contribution of black spruce growing on permafrost peat soils to

275    the overall water flux for a boreal peat landscape. We demonstrate that, while overstory

276    vegetation (i.e., black spruce) is not a significant contributor (<1% of landscape ET flux), the

277    loss of black spruce due to accelerating permafrost thaw could alter the partitioning of energy

278    within this broad landscape. When compared with black spruce growing on mineral soils and/or

279    at lower latitudes, black spruce growing on peat plateaus with permafrost has the lowest sap

280    flow, likely resulting in the minor contribution of overstory to landscape ET. As forested

281    permafrost peat plateaus along the southern limit of permafrost transition into permafrost-free

282    and treeless wetland environments (i.e., bogs and fens), it will become increasingly important to

283    quantify contributions from various shrub species, peatland sedges and mosses, and open water

284    areas.

285

CONTRIBUTION OF OVERSTORY TRANSPIRATION IN A BOREAL PERMAFROST PEATLAND

306   **References**

307   Angstmann, J. L., Ewers, B. E., Barber, J., & Kwon, H. (2013). Testing transpiration controls by

308        quantifying spatial variability along a boreal black spruce forest drainage gradient.

309        *Ecohydrology*, *6*, 783–793. http://doi.org/10.1002/eco.1300

310   Angstmann, J. L., Ewers, B. E., & Kwon, H. (2012). Size-mediated tree transpiration along soil

311        drainage gradients in a boreal black spruce forest wildfire chronosequence. *Tree*

312        *Physiology*, *32*, 599–611. http://doi.org/10.1093/treephys/tps021

313   Baltzer, J. L., Veness, T., Chasmer, L. E., Sniderhan, A. E., & Quinton, W. L. (2014). Forests on

314        thawing permafrost: fragmentation, edge effects, and net forest loss. *Global Change*

315        *Biology*, 824–834. http://doi.org/10.1111/gcb.12349

316   Bonan, G. B. (2008). Forests and climate change: forcings, feedbacks, and the climate benefits of

317        forests. *Science*, *320*, 1444–1449. http://doi.org/10.1126/science.1155121

318   Bovard, B. D., Curtis, P. S., Vogel, C. S., Su, H.-B., & Schmid, H. P. (2005). Environmental

319        controls on sap flow in a northern hardwood forest. *Tree Physiology*, *25*, 31–38.

320   Burgess, S., Adams, M. A., Turner, N. C., Beverly, C. R., Ong, C. K., Khan, A. A., & Bleby, T.

321        M. (2001). An improved heat pulse method to measure low and reverse rates of sap flow in

322        woody plants. *Tree Physiology*, *21*, 589–98.

323   Chasmer, L. E., & Hopkinson, C. (2016). Threshold loss of discontinuous permafrost and

324        landscape evolution. *Global Change Biology*, 1–15. http://doi.org/10.1111/gcb.13537

325   Chasmer, L. E., Hopkinson, C., Veness, T., Quinton, W. L., & Baltzer, J. L. (2014). A decision-

326        tree classification for low-lying complex land cover types within the zone of discontinuous

327        permafrost. *Remote Sensing of Environment*, *143*, 73–84.

328        http://doi.org/10.1016/j.rse.2013.12.016

CONTRIBUTION OF OVERSTORY TRANSPIRATION IN A BOREAL PERMAFROST PEATLAND

329    Chasmer, L. E., Quinton, W. L., Hopkinson, C., Petrone, R. M., & Whittington, P. (2011).

330        Vegetation canopy and radiation controls on permafrost plateau evolution within the

331        discontinuous permafrost zone, Northwest Territories, Canada. *Permafrost and Periglacial*

332        *Processes*, *22*, 199–213. http://doi.org/10.1002/ppp.724

333    Coenders-Gerrits, A. M. J., van der Ent, R. J., Bogaard, T. A., Wang-Erlandsson, L., Hrachowitz,

334        M., & Savenije, H. H. G. (2014). Uncertainties in transpiration estimates. *Nature*, *506*, E1-

335        2. http://doi.org/10.1038/nature12925

336    Connon, R. F., Quinton, W. L., Craig, J. R., & Hayashi, M. (2014). Changing hydrologic

337        connectivity due to permafrost thaw in the lower Liard River valley, NWT, Canada.

338        *Hydrological Processes*. http://doi.org/10.1002/hyp.10206

339    Environment Canada. (2014). *Canadian Climate Normals: 1981–2010*. Available at:

340        http://climate.weather.gc.ca/climate_normals/index_e.html (accessed 7 February 2017).

341    Ewers, B. E., Gower, S. T., Bond-Lamberty, B., & Wang, C. K. (2005). Effects of stand age and

342        tree species on canopy transpiration and average stomatal conductance of boreal forests.

343        *Plant, Cell and Environment*, *28*, 660–678. http://doi.org/10.1111/j.1365-

344        3040.2005.01312.x

345    Fatichi, S., and C. Pappas. (2017). Constrained variability of modeled T:ET ratio across biomes.

346        *Geophysical Research Letters*, *44*, doi:10.1002/2017GL074041.

347    Fatichi, S., C. Pappas, and V. Y. Ivanov. (2015). Modeling plant-water interactions: an

348        ecohydrological overview from the cell to the global scale. *Wiley Interdisciplinary Reviews*

349        *Water*, *3*(3), 327–368, doi:10.1002/wat2.1125

350    Finger, R. A., Turetsky, M. R., Kielland, K., Ruess, R. W., Mack, M. C., & Euskirchen, E. S.

351        (2016). Effects of permafrost thaw on nitrogen availability and plant-soil interactions in a

17

352    boreal Alaskan lowland. *Journal of Ecology*, *104*(6), 1542–1554.

353    http://doi.org/10.1111/1365-2745.12639

354  Gale, M. R., & Grigal, D. F. (1987). Vertical root distribution of northern tree species in relation

355    to successional status. *Canadian Journal of Forest Research*, *17*, 829–834.

356  Garon-Labrecque, M.-E., Leveille-Bourret, E., Higgins, K., & Sonnentag, O. (2015). Additions

357    to the boreal flora of the Northwest Territories with a preliminary vascular flora of Scotty

358    creek. *Canadian Field-Naturalist*, *129*, 349–367.

359  Good, S. P., Noone, D., & Bowen, G. (2015). Hydrological connectivity constrains partitioning

360    of global terrestrial water fluxes. *Science*, *349*, 175–177.

361  Grosse, G., Goetz, S., McGuire, A. D., Romanovsky, V. E., & Schuur, E. A. G. (2016).

362    Changing permafrost in a warming world and feedbacks to the Earth system. *Environmental*

363    *Research Letters*, *11*, 40201. http://doi.org/10.1088/1748-9326/11/4/040201

364  Helbig, M., Pappas, C., & Sonnentag, O. (2016a). Permafrost thaw and wildfire: equally

365    important drivers of boreal tree cover changes across the Taiga Plains, Canada. *Geophysical*

366    *Research Letters*. http://doi.org/10.1002/2015GL067193

367  Helbig, M., Wischnewski, K., Kljun, N., Chasmer, L. E., Quinton, W. L., Detto, M., &

368    Sonnentag, O. (2016b). Regional atmospheric cooling and wetting effect of permafrost

369    thaw-induced boreal forest loss. *Global Change Biology*, 1–19.

370    http://doi.org/10.1111/gcb.13348

371  Hopkinson, C., Chasmer, L. E., Sass, G., Creed, I. F., Sitar, M., Kalbfleisch, W., & Treitz, P.

372    (2005). Vegetation class dependent errors in lidar ground elevation and canopy height

373    estimates in a boreal wetland environment. *Canadian Journal of Remote Sensing*, *31*, 191–

374    206. http://doi.org/10.5589/m05-007

CONTRIBUTION OF OVERSTORY TRANSPIRATION IN A BOREAL PERMAFROST PEATLAND

375  Iijima, Y., Ohta, T., Kotani, A., Fedorov, A. N., Kodama, Y., & Maximov, T. C. (2014). Sap

376      flow changes in relation to permafrost degradation under increasing precipitation in an

377      eastern Siberian larch forest. *Ecohydrology*, *7*, 177–187. http://doi.org/10.1002/eco.1366

378  Jasechko, S., Sharp, Z. D., Gibson, J. J., Birks, S. J., Yi, Y., & Fawcett, P. J. (2013). Terrestrial

379      water fluxes dominated by transpiration. *Nature*, *496*, 347–50.

380      http://doi.org/10.1038/nature11983

381  Jorgenson, M. T., Harden, J., Kanevskiy, M., O'Donnell, J., Wickland, K., Ewing, S., Manies,

382      K., Zhuang, Q., Shur, Y., Striegl, R., & Koch, J. (2013). Reorganization of vegetation,

383      hydrology and soil carbon after permafrost degradation across heterogeneous boreal

384      landscapes. *Environmental Research Letters*, *8*, 35017. http://doi.org/10.1088/1748-

385      9326/8/3/035017

386  Kljun, N., Calanca, P., Rotach, M. W., & Schmid, H. P. (2015). A simple two-dimensional

387      parameterisation for Flux Footprint Prediction (FFP). *Geoscientific Model Development*, *8*,

388      3695–3713. http://doi.org/10.5194/gmd-8-3695-2015

389  Lafleur, P. M. (1992). Energy balance and evapotranspiration from a subarctic forest.

390      *Agricultural and Forest Meteorology*, *58*, 163–175.

391  Lara, M. J., Genet, H., Mcguire, A. D., Euskirchen, E. S., Zhang, Y., Brown, D. R. N., Jorgenson

392      M. T., Romanovsky V. E., Breen A., & Bolton, W. R. (2016). Thermokarst rates intensify

393      due to climate change and forest fragmentation in an Alaskan boreal forest lowland. *Global

394      Change Biology*, *22*, 816–829. http://doi.org/10.1111/gcb.13124

395  Lawrence, D. M., Thornton, P. E., Oleson, K. W., & Bonan, G. B. (2007). The partitioning of

396      evapotranspiration into transpiration, soil evaporation, and canopy evaporation in a GCM:

397      impacts on land–atmosphere interaction. *Journal of Hydrometeorology*, *8*, 862–880.

19

398    http://doi.org/10.1175/JHM596.1

399  National Wetlands Working Group. (1997). *The Canadian wetland classification system*. (B. G.

400    Warner & C. D. A. Rubec, Eds.) *National Wetlands Working Group*. Waterloo, Ontario:

401    Wetlands Research Branch, University of Waterloo.

402  Olefeldt, D., Goswami, S., Grosse, G., Hayes, D., Hugelius, G., Kuhry, P., McGuire, A. D.,

403    Romanovsky, V. E., Sannel, A. B. K., Schuur, E. A. G., & Turetsky, M. R. (2016).

404    Circumpolar distribution and carbon storage of thermokarst landscapes. *Nature*

405    *Communications*, *7*, 13043. http://doi.org/10.1038/ncomms13043

406  Oren, R., & Pataki, D. E. (2001). Transpiration in response to variation in microclimate and soil

407    moisture in southeastern deciduous forests. *Oecologia*, *127*, 549–559.

408    http://doi.org/10.1007/S004420000622

409  Patankar, R., Quinton, W. L., Hayashi, M., & Baltzer, J. L. (2015). Sap flow responses to

410    seasonal thaw and permafrost degradation in a subarctic boreal peatland. *Trees - Structure*

411    *and Function*, *29*, 129–142. http://doi.org/10.1007/s00468-014-1097-8

412  Quinton, W. L., Hayashi, M., & Chasmer, L. E. (2011). Permafrost-thaw-induced land-cover

413    change in the Canadian subarctic: implications for water resources. *Hydrological Processes*,

414    *25*, 152–158. http://doi.org/10.1002/hyp.7894

415  Schaefer, K., Lantuit, H., Romanovsky, V. E., & Schuur, E. A. G. (2012). Policy Implications of

416    Warming Permafrost. *United Nations Environment Programme Special Report*.

417  Schlesinger, W. H., & Jasechko, S. (2014). Transpiration in the global water cycle. *Agricultural*

418    *and Forest Meteorology*, *189–190*, 115–117. http://doi.org/10.1016/j.agrformet.2014.01.011

419  Smith, S. L., Burgess, M. M., Riseborough, D., & Mark Nixon, F. (2005). Recent trends from

420    Canadian permafrost thermal monitoring network sites. *Permafrost and Periglacial*

421    *Processes*, *16*, 19–30. http://doi.org/10.1002/ppp.511

422    Sniderhan, A. E., & Baltzer, J. L. (2016). Growth dynamics of black spruce (Picea mariana) in a

423         rapidly thawing discontinuous permafrost peatland. *Journal of Geophysical Research:*

424         *Biogeosciences*, *121*, 2988–3000. http://doi.org/10.1002/2016JG003528

425    Sonnentag, O., Talbot, J., Chen, J. M., & Roulet, N. T. (2007). Using direct and indirect

426         measurements of leaf area index to characterize the shrub canopy in an ombrotrophic

427         peatland. *Agricultural and Forest Meteorology*, *144*, 200–212.

428         http://doi.org/10.1016/j.agrformet.2007.03.001

429    Sprugel, D. G. (1983). Correcting for bias in log-transformed allometric equations. *Ecology*.

430         http://doi.org/10.2307/1937343

431    Steppe, K., De Pauw, D. J. W., Doody, T. M., & Teskey, R. O. (2010). A comparison of sap flux

432         density using thermal dissipation, heat pulse velocity and heat field deformation methods.

433         *Agricultural and Forest Meteorology*, *150*, 1046–1056.

434         http://doi.org/10.1016/j.agrformet.2010.04.004

435    Tarnocai, C., Kettles, I. M., & Lacelle, B. (2005). *Peatlands of Canada Database*. Geological

436         Survey of Canada.

437    Turetsky, M. R., Wieder, K., & Vitt, D. H. (2002). Boreal peatland C fluxes under varying

438         permafrost regimes. *Soil Biology and Biochemistry*, *34*, 907–912.

439         http://doi.org/10.1016/S0038-0717(02)00022-6

440    Van Herk, I. G., Gower, S. T., Bronson, D. R., & Tanner, M. S. (2011). Effects of climate

441         warming on canopy water dynamics of a boreal black spruce plantation. *Canadian Journal*

442         *of Forest Research*, *41*, 217–227. http://doi.org/10.1139/X10-196

443    Wang, K., & Dickinson, R. E. (2012). A review of global terrestrial evapotranspiration:

21

CONTRIBUTION OF OVERSTORY TRANSPIRATION IN A BOREAL PERMAFROST PEATLAND

444     observation, modelling, climatology, and climatic variability. *Review of Geophysics*, *50*, 1–

445     54. http://doi.org/10.1029/2011RG000373

446     Wang, L., Good, S. P., & Caylor, K. K. (2014). Global synthesis of vegetation control on

447     evapotranspiration partitioning. *Geophysical Research Letters*, 6753–7657.

448     http://doi.org/10.1002/2014GL061439

449     Zoltai, S. C., & Tarnocai, C. (1975). Perennially frozen peatlands in the Western Arctic and

450     Subarctic of Canada. *Canadian Journal of Earth Science*, *12*, 28–43.

451

22

CONTRIBUTION OF OVERSTORY TRANSPIRATION IN A BOREAL PERMAFROST PEATLAND

1
2
3
4   452   **Table 1.** A non-exhaustive literature review of reported values of black spruce sap flux density
5
6   453   in the boreal region, including study location, soil type, permafrost presence (PF, Yes/No), tree
7
8   454   sap flux density ($J_S$ in $gH_20$ m$^{-2}$ s$^{-1}$), diameter at breast height (DBH, cm), mean tree height ($H$,
9
10
11  455   m), sapwood area ($A_S$, cm$^2$), stem density (D, stems m$^{-2}$), leaf area index (LAI, m$^2$ m$^{-2}$), air
12
13  456   temperature (°C) and mean annual precipitation (Prec., mm).
14
15  457
16
17  458
18
19  459
20
21  460
22
23  461
24
25  462
26
27  463
28
29  464
30
31  465
32
33  466
34
35  467
36
37  468
38
39  469
40
41  470
42
43  471
44
45  472
46
47  473
48
49  474
50
51  475
52
53
54
55
56
57
58
59
60                                                                                                    23

CONTRIBUTION OF OVERSTORY TRANSPIRATION IN A BOREAL PERMAFROST PEATLAND

| Study | Location | Soil | PF | n | $J_S$ | DBH | H | $A_S$ | D | LAI | T | Prec. |
|---|---|---|---|---|---|---|---|---|---|---|---|---|
| This study (SFS) | 61°180'N, 121°180'W | peat | Y | 22 | 8.0[a] | 10.6 | - | - | - | - | - | 88.8 |
| This study (CHM) | 61°180'N, 121°180'W | peat | Y | - | - | 2.8 | 2.2 | 1.8 | 0.12 | 0.6 | -2.7 | 390 |
| Angstmann *et al.* (2013) | 55°55'N, 98°21'W | peat | N | 117 | 18.0[b] | - | - | 2.1 | 0.48 | 2.7[*] | 0.8 | 439 |
| Van Herk *et al.* (2011) | 55°53'N, 98°20'W | mineral | N | 16 | 61.5[c] | 5.5 | - | 2.7 | 0.20 | 3.1 | -3.2 | 517 |
| Ewers *et al.* (2005) | 55°53'N, 98°20'W | mineral | N | 38 | 86.7[d] | 6.9 | 6.9 | - | 0.39 | 3.6 | 0.8 | 439 |

[*] from Angstmann *et al.* (2012)

Superscripts refer to the time period over which mean $J_S$ was calculated: [a] over 24 h period $0000 - 2359$ h June - July, [b] over 12 h period $0600 - 1800$ h; mean of all stands, [c] over 24 h period May – September; mean given for outside control trees (CO) only, [d] over 24 h period from 0500 h of one day to 0430 h the next day June - September; value of $J_S$ reported given by Van Herk *et al.* (2011) for Ewers *et al.* (2005).

476
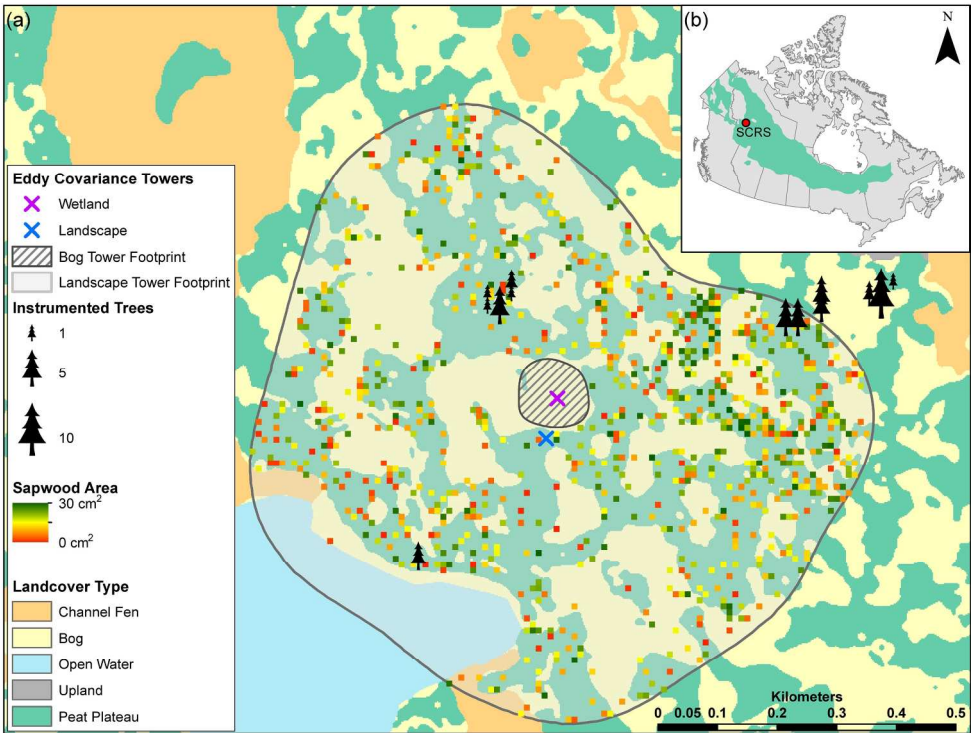
Figure 1. (a) Land cover classes at the study area (Chasmer *et al*., 2014). The approximate locations and number of sap flow sensors are denoted by tree symbols of different sizes (note symbols appearing to be located in wetlands are the result of mapping limitations and are in fact located on plateaus). The locations of the landscape ($ET_{LAND}$) and wetland ($ET_{BOG}$) eddy covariance towers, with the solid and hatched shaded areas corresponding to the growing season flux footprint of the landscape and wetland towers respectively. The coloured cells illustrate the distribution of sapwood area ($cm^2$) derived from a 1 m resolution canopy height model and empirical allometric relationships resampled to 10 m resolution for figure's clarity. (b) Spatial extent of peatlands occurring within the boreal zone extracted from the Peatlands of Canada database (Tarnocai *et al*., 2005) and consisting of landscapes characterized by permafrost-free channel fens, bogs and black spruce forested permafrost peat plateaus as described by (Zoltai and Tarnocai, 1975), and the location of the Scotty Creek Research Station (ScCr).

215x166mm (300 x 300 DPI)
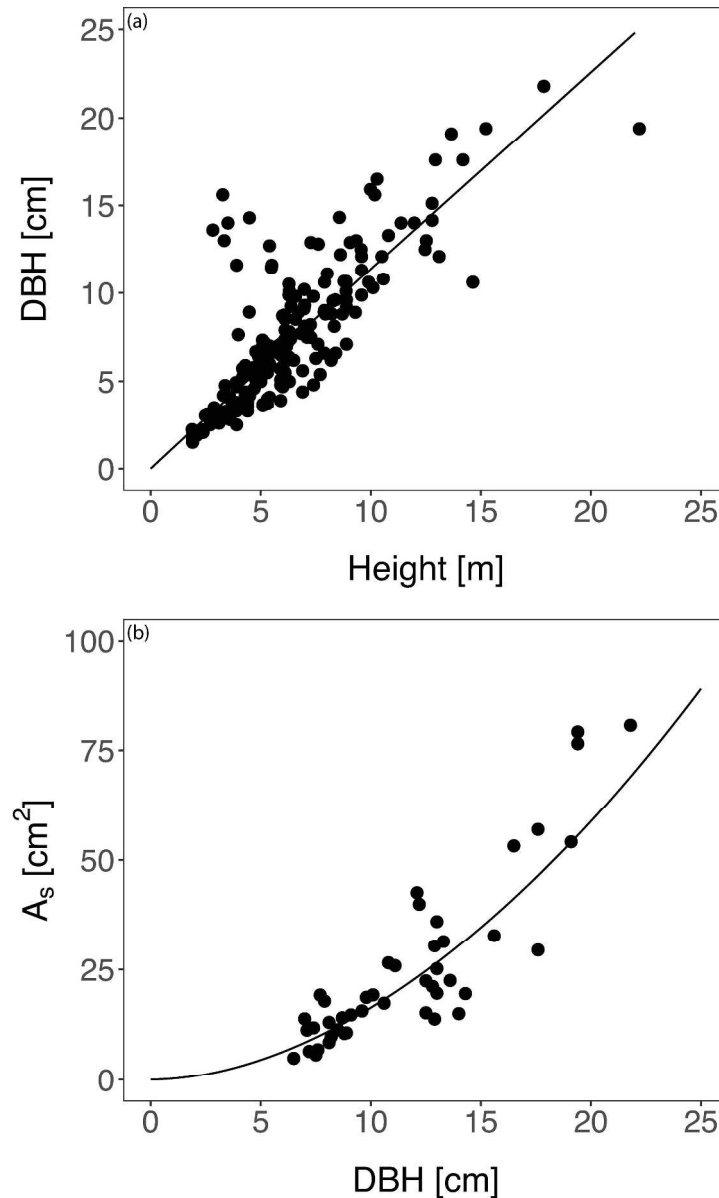
Figure 2. Allometric relationships between (a) tree height (m) and diameter at breast height (cm) based on 198 trees measured within the landscape eddy covariance footprint at Scotty Creek in 2012, 2015, and 2016 and (b) diameter at breast height (cm) and sapwood area (cm$^2$) based on 47 trees measured within the landscape eddy covariance footprint at Scotty Creek in 2016.
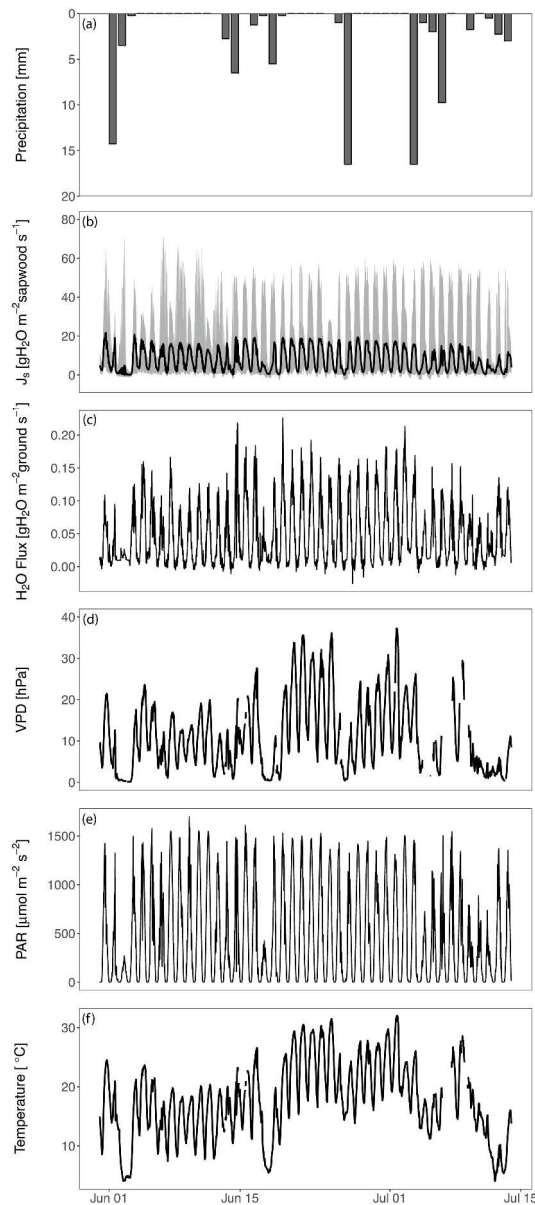
245x409mm (300 x 300 DPI)

Figure 3. (a) Daily total precipitation at Scotty Creek over the 2013 study period. (b) Average ($n$ = 22) $J_S$ (black), and the minimum and maximum flux (grey). (c) Evapotranspiration of the forest-wetland landscape ($ET_{LAND}$), (d) vapour pressure deficit (VPD), (e) photosynthetically active radiation (PAR) and (f) 2 m air temperature recorded at the landscape eddy covariance tower over the study period.

535x1218mm (300 x 300 DPI)
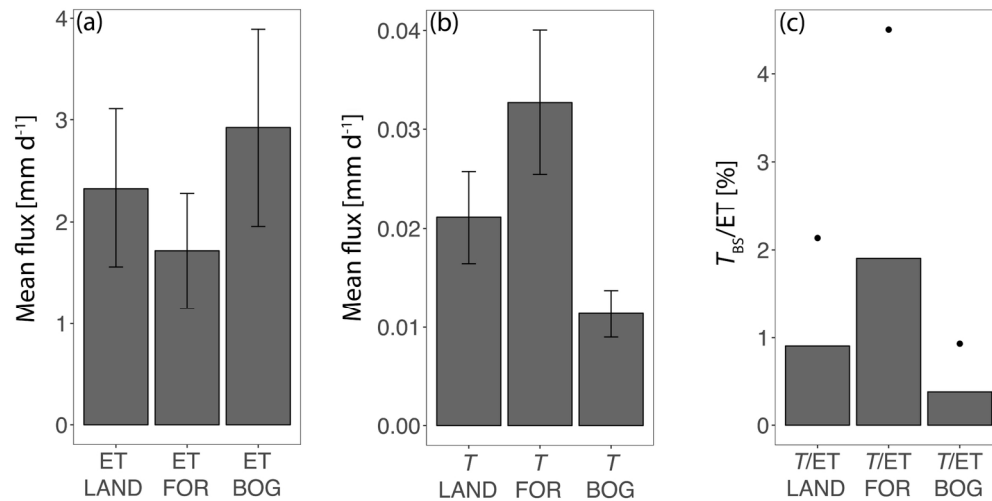
Figure 4. (a) Evapotranspiration (ET) for different landcover types, namely landscape (LAND), forest (FOR) and wetlands (BOG) for 2013 based on data from the landscape eddy covariance tower. Vertical lines correspond to ± one standard deviation. (b) Upscaled landscape, forest and wetland transpiration ($T_{BS}$) using tree level sap flux density measurements. Vertical lines correspond ± one standard deviation on the Monte Carlo uncertainty analysis. (c) The contribution of black spruce transpiration to evapotranspiration ($T_{BS}$/ET x 100%) for the different landcover types (e.g. landscape, forest, wetland) in 2013. Points represent the upper limit of $T_{BS}$ assuming trees ≤5.4 cm at breast height are entirely composed of conducting tissue and trees >5.4 cm at breast height have a sapwood area equal to half the cross sectional area.
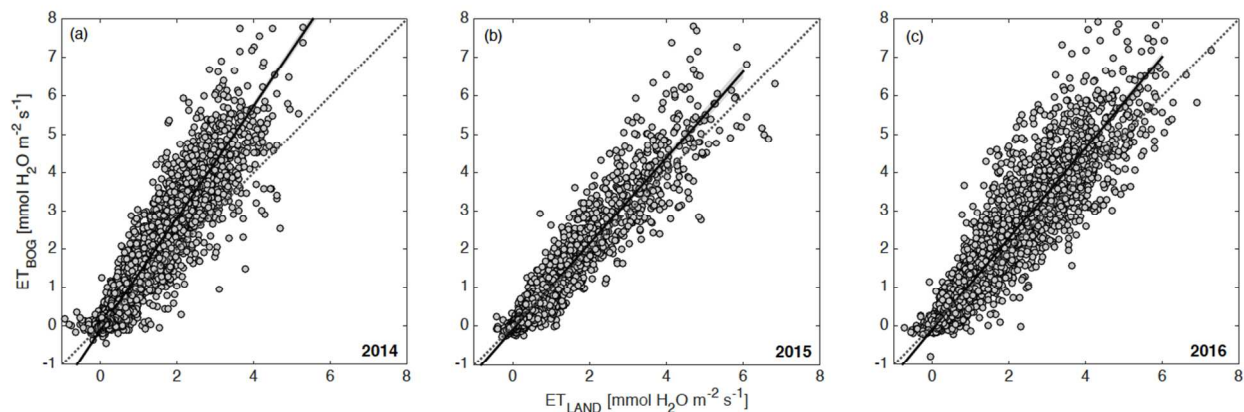
158x79mm (300 x 300 DPI)

**Figure S1.** Relationship between landscape ($ET_{LAND}$) and wetland ($ET_{BOG}$) half-hourly water

flux measured at Scotty Creek in (a) 2014, (b) 2015) and (c) 2016. The mean slope and intercept

for the three-year period was used to calculate $ET_{BOG}$ in 2013 when it was not measured.
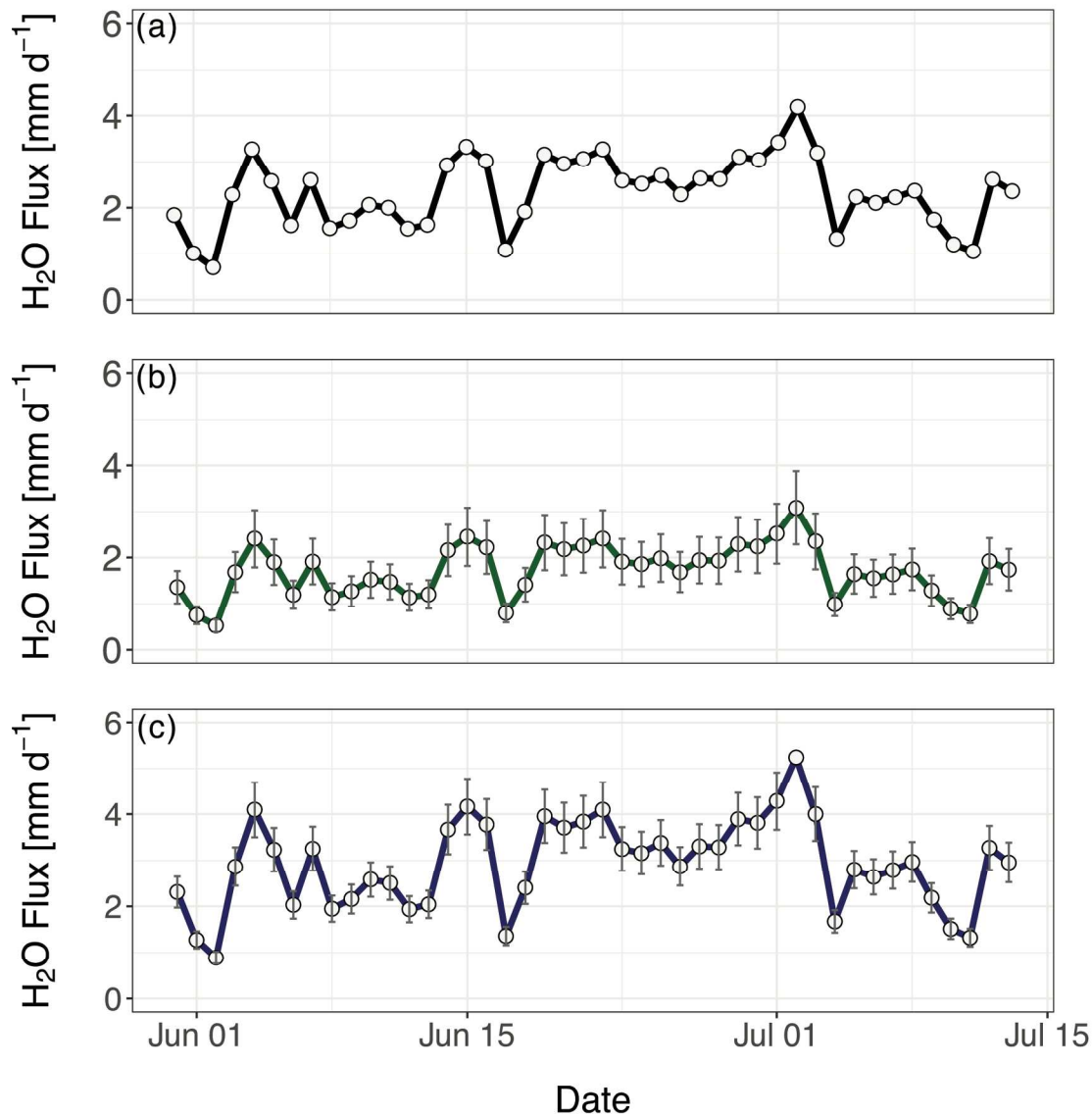
**Figure S1.** (a) Daily total landscape water flux ($ET_{LAND}$) measured at the landscape eddy

covariance tower at Scotty Creek during the 2013 study period. (b) Daily total forest (i.e.,

plateau) water flux ($ET_{FOR}$) derived as the residual from $ET_{LAND}$ and the wetland water flux

($ET_{BOG}$). Error bars refer to the confidence intervals of the derived residuals. (c) Daily total

$ET_{BOG}$ derived from the mean slope and intercept of the relationship between $ET_{LAND}$ and $ET_{BOG}$

2014 – 2016 at Scotty Creek. Error bars refer to the confidence interval of the derived estimates.
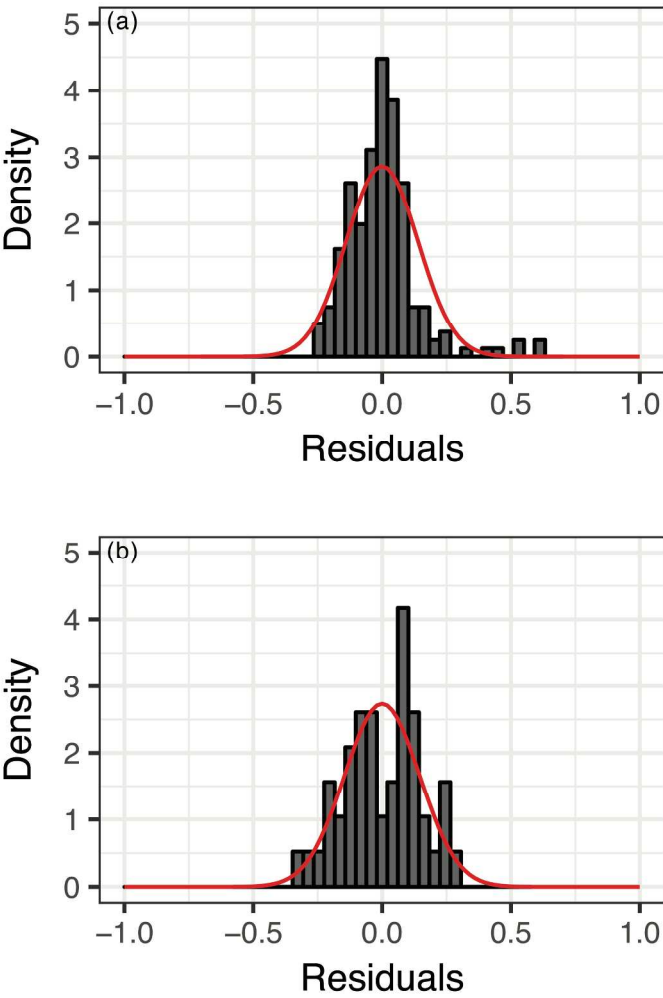
**Figure S3:** Probability density of the residuals resulting from the power function defining the

relationship between (a) tree height and diameter at breast height and, (b) diameter at breast

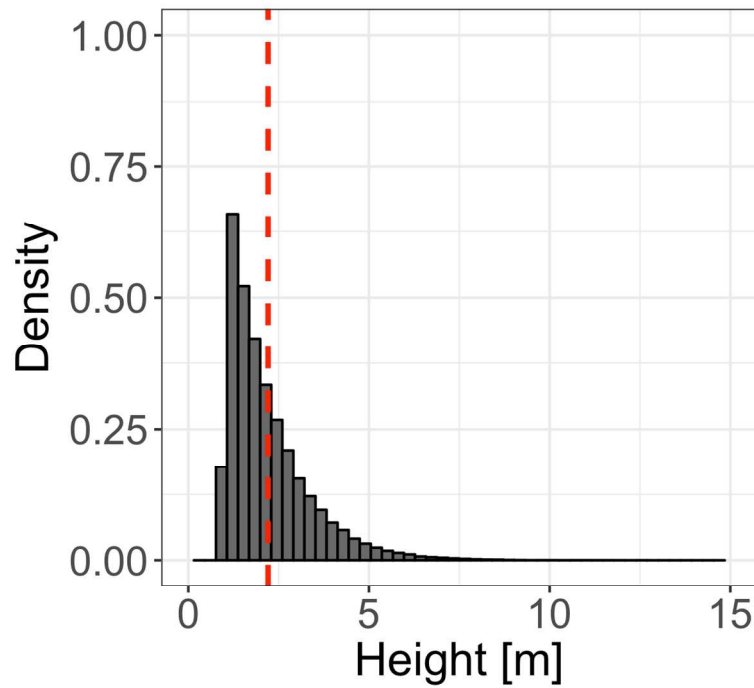height and sapwood area at Scotty Creek. The residuals conform to a normal distribution.

**Figure S4.** Distribution of tree height (m) within the landscape eddy covariance footprint at

Scotty Creek, extracted from the CHM. Average tree height was determined to be 2.2 m +/- 1.2

(shown in red; minimum = 1.0 m, maximum = 12.6 m), and was not measured for the
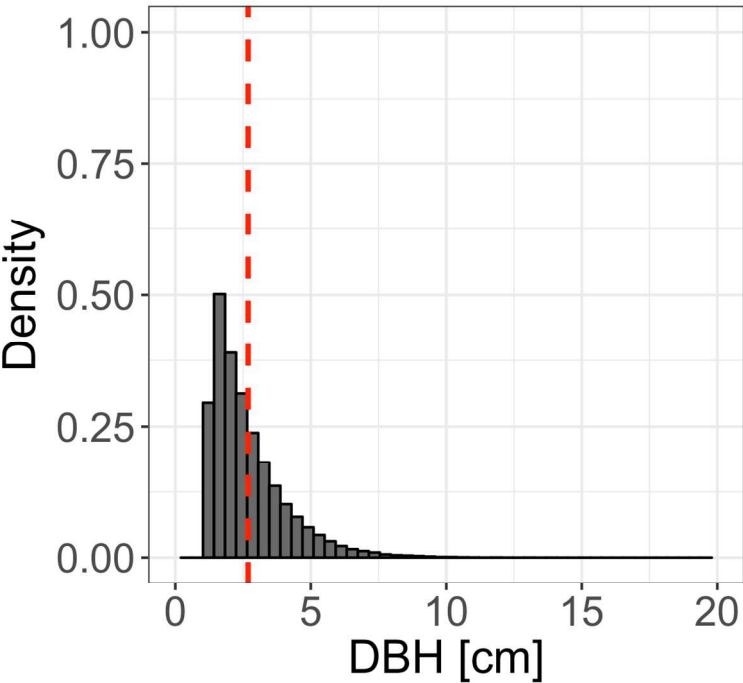
instrumented trees.

**Figure S5.** Distribution of DBH (cm) within the landscape eddy covariance footprint at Scotty

Creek, estimated allometrically from the relationship between the measured trees and CHM.

Average DBH was determined to be 2.7 cm +/- 1.4 (shown in red; minimum = 1.2 cm, maximum

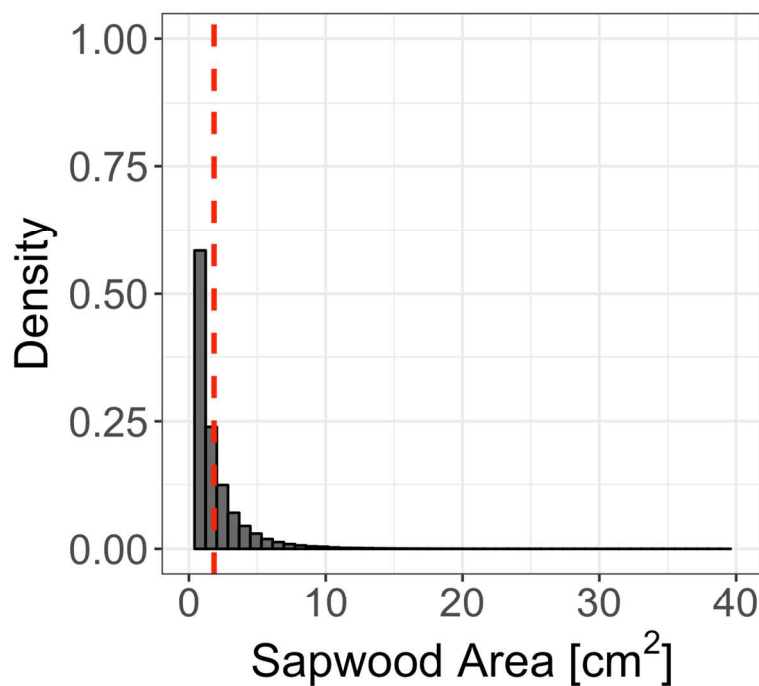= 15.1 cm), in contrast to 10.6 cm +/- 0.5 for the instrumented trees.

**Figure S6.** Distribution of sapwood area ($cm^2$) within the landscape eddy covariance footprint at

Scotty Creek, estimated allometrically from the relationship between the measured trees and

CHM. Average sapwood area was determined to be 1.8 $cm^2$ +/- 2.0 (shown in red; minimum =

0.4 $cm^2$, maximum = 37.1 $cm^2$), and was not measured for the instrumented trees.